

Optimization of Nasopharyngeal carcinoma (NPC) spheroid formation for 5-ALA PDT study

Wu, R.W.K.; Chu, E.S.M.; Yuen, J.Y.M.; Huang, Z.

Published in:
Photodiagnosis and Photodynamic Therapy

DOI:
[10.1016/j.pdpdt.2024.104185](https://doi.org/10.1016/j.pdpdt.2024.104185)

Publication date:
2024

Document Version
Publisher's PDF, also known as Version of record

[Link to publication in ResearchOnline](#)

Citation for published version (Harvard):
Wu, RWK, Chu, ESM, Yuen, JYM & Huang, Z 2024, 'Optimization of Nasopharyngeal carcinoma (NPC) spheroid formation for 5-ALA PDT study', *Photodiagnosis and Photodynamic Therapy*, vol. 46, 104185. <https://doi.org/10.1016/j.pdpdt.2024.104185>

General rights

Copyright and moral rights for the publications made accessible in the public portal are retained by the authors and/or other copyright owners and it is a condition of accessing publications that users recognise and abide by the legal requirements associated with these rights.

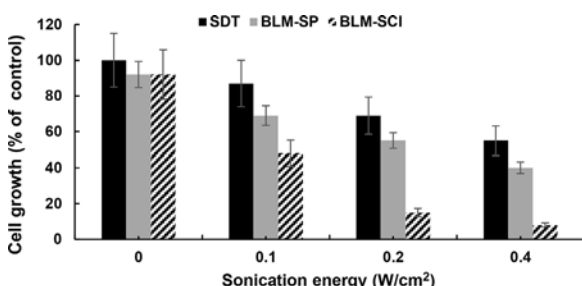
Take down policy

If you believe that this document breaches copyright please view our takedown policy at <https://edshare.gcu.ac.uk/id/eprint/5179> for details of how to contact us.

Non treatment controls, 2) BLM “dark” control, and 3) BLM-SCI. 1×10^5 , (pre-incubated with BLM) Mat B III tumor cells, suspended in $100 \mu\text{l}$, were implanted orthotopically into the right axillar mammary fat pad. Sonication at either 0.4, 0.8, and 2 W/cm^2 was commenced shortly after cell injection and administered for 5 minutes via a 1-cm diameter US transducer centered over the injection site. All animals were sacrificed on day 14 post implantation, and the tumors were surgically removed, and their volume measured.

4. Results

The effects of BLM-SCI, *in vitro*, on the growth of Mat B III monolayers is shown in the figure. Control cells treated with SDT or BLM-SP (sonoporation) demonstrated growth inhibition but could not completely inhibit growth. In contrast, tumor cells treated with BLM-SCI showed a 95% reduction in growth at the highest sonication (0.4 W/cm^2).



The development of Mat B III tumors *in vivo*, following treatment, is shown in the table below.

Treatment	None	BLM	BLM-SCI 0.4W	BLM-SCI 0.8W	BLM-SCI 2W
Tumor volume*	2100	1700	800	600	125

*Tumor volume in mm^3

The average tumor size in the BLM-only control group was smaller than the non-treated control group, but the difference was not significant. In contrast, the average tumor volumes in the three BLM-SCI groups were significantly less than the average volumes in the NTC or BLM controls. The inhibitory effects of BLM-PCI clearly increased with the sonication energy level, and three of the six animals in the 2 W/cm^2 cohort did not develop any visible tumors at harvest.

5. Conclusion

Advantages of ultrasound over light activation are non-invasive treatment protocols, and greatly increased depth of therapy. Since even moderate US energy levels, like 0.8 W/cm^2 , in the animal model used, could reduce resultant tumor size by 75% with a single treatment, the non-invasiveness and its external mode of application of US would allow for fractionated and repetitive treatment. This is an important advantage when translating to clinical protocols.

Acknowledgments

The authors are grateful for support from the Norwegian Radium Hospital Research Foundation.

Reference

[1]. Hirschberg H, Madsen SJ. Synergistic efficacy of ultrasound, sonosensitizers and chemotherapy: a review. *Ther Deliv.* 2017 May;8(5):331-42.

doi: [10.1016/j.pdpdt.2024.104184](https://doi.org/10.1016/j.pdpdt.2024.104184)

Optimization of Nasopharyngeal carcinoma (NPC) spheroid formation for 5-ALA PDT study

RWK WU^a, ESM CHU^b, JYM YUEN^c, Z HUANG^d

^a Department of Biological and Biomedical Sciences, School of Health and Life Sciences, Glasgow Caledonian University, Glasgow, Scotland, UK

^b School of Medical and Health Sciences, Tung Wah College, HKSAR, China

^c School of Nursing, The Hong Kong Polytechnic University, HKSAR, China

^d MOE Key Laboratory of Photonics Science and Technology for Medicine, Fujian Normal University, Fuzhou, China

Significance: Recently, there is an increase in PDT studies using 3D spheroids. However, there is limited information demonstrating the effect of spheroid size on PDT study. This study aims to provide information on the effect of NPC/CNE2 spheroid size on PpIX accumulation and PDT efficacy.

Approach: NPC/CNE2 spheroids were generated with different initial cell densities (5,000-60,000 cells/well). Spheroids' diameter and morphological characteristics were recorded for 5 days and post-PDT 24-72 hours. The intracellular PpIX accumulation was measured by the Incucyte S3 live-cell analysis system.

Results: Spheroid size increased with initial cell density. Spheroids formed within 5,000-20,000 cells were less varied in size and with smooth round edges. The PpIX accumulation was spheroid size-dependent with PpIX accumulation increased in larger spheroids. 5-ALA-PDT inhibited spheroid growth with a decrease in size of periphery compared to the control.

Conclusions: The spheroid size is an important factor affects *in vitro* PDT study.

Keywords: 3D spheroids, spheroid size, initial cell density, PpIX accumulation, 5-ALA

1. Introduction and Background

3D spheroids are accepted as more physiologically relevant cell culture models for PDT anti-cancer studies [1]. Recently, there is an increase in using 3D spheroids to study PDT anti-tumour efficacy on cancers [2-6]. It is accepted that the spheroid architecture affects the biodistribution of photosensitizers, light penetration, and oxygen level [7-8]. We previously developed NPC 3D spheroids with different techniques resulting in different spheroid diameters ranging from $540 \mu\text{m}$ - $662 \mu\text{m}$ in diameter [9]. However, there is no information on how the spheroid size affects the distribution of photosensitizers.

2. Aims

This study aims to reveal the effect of spheroid size generated from different initial cell densities on PpIX accumulation and PDT efficacy using NPC/CNE2 cell line.

3. Methods

NPC/CNE2 spheroids were generated using the scaffold-free liquid overlay method. In brief, 96 well ultra-low adhesive plates were used and NPC/CNE2 cells with different initial cell densities ranging from 5,000 to 60,000 cells/well were seeded and grown for 5 days. The effect of different initial cell densities on spheroid size was measured by the changes in spheroids' diameter and morphological characteristics using ImageJ. The intracellular PpIX accumulation was measured by the Incucyte S3 live-cell analysis system. In brief, spheroids with selected initial cell densities (5,000, 10,000, 20,000, 30,000 and 60,000 cells) were grown for 3 days. Spheroids were incubated with 1 mM ALA at 0-26 hours.

The PDT efficacy on NPC/CNE2 spheroids was measured by the changes in spheroids' core and periphery size and morphological characteristics. Actively proliferating cells formed the periphery zone in the spheroid. Spheroids cultured at day 3 were incubated with 1 mM 5-ALA for 24

hours, followed by 3J light activation. The changes in spheroids' size and morphological characteristics at post-PDT 24 hours and 72 hours.

4. Results

The spheroid size increased from $393.7\mu\text{m}\pm 15.7\mu\text{m}$ to $944.6\mu\text{m}\pm 81.4\mu\text{m}$ with the initial cell densities increased from 5,000 to 60,000 cells/well at day 3 culture. Spheroids formed by 5,000-20,000 cells were less varied in size and with smooth round edges, while spheroids formed by 30,000 and 60,000 cells were observed with irregular edges and a dense core.

The PpIX accumulation was spheroid size dependent, with an increase of PpIX accumulation in larger spheroids. Interestingly, PpIX accumulation started from the peripheral regions to the core in small spheroids, with maximum PpIX accumulation at the core at 26 hours of incubation. However, the PpIX accumulation in large spheroids mainly remained in the peripheral regions. This finding could be explained by the densities of spheroids and the diffusion distance as 5-ALA are more difficult to diffuse into the core of the spheroids when the spheroid size and volume increase.

1mM 5-ALA-PDT with 3J light activation showed an inhibitory effect on spheroids formed by 5,000 and 30,000 cells. For post-PDT 24 to 72 hours, the periphery size of control spheroids formed by 5,000 and 30,000 cells increased from $83.9\mu\text{m}\pm 25.3\mu\text{m}$ to $103.1\mu\text{m}\pm 33.9\mu\text{m}$ and from $111.0\mu\text{m}\pm 32.2\mu\text{m}$ to $131.1\mu\text{m}\pm 42.3\mu\text{m}$, respectively. However, the periphery size was inhibited by 5-ALA-PDT on PDT-treated spheroids formed by 5,000 and 30,000 cells, with a decrease from $84.5\mu\text{m}\pm 26.2\mu\text{m}$ to $59.0\mu\text{m}\pm 23.7\mu\text{m}$ and from $99.8\mu\text{m}\pm 45.3\mu\text{m}$ to $97.0\mu\text{m}\pm 46.6\mu\text{m}$, respectively. Loose structures with cells disaggregated from the spheroids were also observed in PDT-treated spheroids.

5. Conclusion

The NPC/CNE2 spheroids with different sizes can be formed by different initial cell densities. The size of spheroids affects the PpIX accumulation and PDT efficacy. More in-depth studies are deserved for the optimization of NPC/CNE2 3D spheroid formation for PDT studies.

Disclosures if required

The authors confirmed that there are no conflicts of interest should be declared.

Acknowledgement

The authors thank SARTORIUS for kindly providing the Incucyte S3 system with technical support to the system for the study.

References

- [1] L. Mohammad-Hadi, A.J. MacRobert, M. Loizidou, E. Yaghini. Photodynamic therapy in 3D cancer models and the utilization of nanodelivery systems. *Nanoscale*. (2018) 10(4): 1570-1581. doi:10.1039/c7nr07739d.
- [2] M.B. Gariboldi, E. Marras, I. Vaghi, A. Margheritis, M.C. Malacarne, E. Caruso, Phototoxicity of two positive-charged diaryl porphyrins in multicellular tumor spheroids, *J Photochem Photobiol B*. (2021) 225:112353. https://doi.org/10.1016/j.jphotobiol.2021.112353.
- [3] C.C. Chuang, Y.N. Chen, Y.Y. Wang, Y.C. Huang, S.Y. Lin, R.Y. Huang, Y.Y. Jang, C.C. Yang, Y.F. Huang, C.W. Chang, Stem Cell-Based Delivery of Gold/Chlorin e6 Nanocomplexes for Combined Photothermal and Photodynamic Therapy, *ACS Appl Mater Interfaces*. (2020) 12(27):30021-30030. https://doi.org/10.1021/acsami.0c03446.
- [4] M.S. Mathews, J.W. Blickenstaff, E.-C. Shih, G. Zamora, V. Vo, C.-H. Sun, H. Hirschberg, S.J. Madsen, Photochemical internal-

ization of bleomycin for glioma treatment, *J Biomed Opt*. (2012) 17(5):058001. https://doi.org/10.1117/1.jbo.17.5.058001.

- [5] C.L. Evans, A.O. Abu-Yousif, Y.J. Park, O.J. Klein, J.P. Celli, I. Rizvi, X. Zheng, T. Hasan, Killing hypoxic cell populations in a 3D tumor model with EtNBS-PDT, *PLoS One*. (2011) 6(8):e23434. https://doi.org/10.1371/journal.pone.0023434.
- [6] M. Broekgaarden, A.L. Bulin, J. Frederick, Z. Mai, T. Hasan, Tracking photodynamic- and chemotherapy-induced redox-state perturbations in 3D culture models of pancreatic cancer: A tool for identifying therapy-induced metabolic changes, *J Clin Med*. (2019) 8(9):1399. https://doi.org/10.3390/jcm8091399.
- [7] S. Maji, H. Lee, Engineering Hydrogels for the Development of Three-Dimensional In Vitro Models. *Int J Mol Sci*. (2022) 23(5): 2662. https://doi.org/10.3390/ijms23052662.
- [8] O. Habanjar, M. Diab-Assaf, F. Caldefie-Chezet, L. Delort, 3D cell culture systems: Tumor application, advantages, and disadvantages. *Int J Mol Sci*. (2021) 22(22): 12200. https://doi.org/10.3390/ijms222212200.
- [9] R.W.K. Wu, E.S.M. Chu, J. W. M. Yuen, Z. Huang. Comparative study of FosPeg® photodynamic effect on nasopharyngeal carcinoma cells in 2D and 3D models. *J Photochem Photobiol B*. (2020) 210:111987. doi:10.1016/j.jphotobiol.2020.111987.

doi: 10.1016/j.jpdpdt.2024.104185

Potential therapeutic efficacy of Photodynamic Therapy on triple negative breast cancer in hormonal microenvironment

KCN Cheung^a, GMN Leung^a, RWK Wu^b, JWM Yuen^c, Z Huang^d, ESM Chu^a

^aSchool of Medical and Health Sciences, Tung Wah College, Hong Kong SAR

^bDepartment of Biological and Biomedical Sciences, School of Health and Life Sciences, Glasgow Caledonian University, Glasgow, Scotland, United Kingdom

^cSchool of Nursing, Hong Kong Polytechnic University, Hong Kong SAR

^dMOE Key Laboratory of Photonics Science and Technology for Medicine, Fujian Normal University, Fuzhou, China

Significance: There are seldom studies on the determination of cancer treatment efficacy related to normal hormonal tumor microenvironment on triple negative breast cancer (TNBC). This study aimed to determine Hexyl-ALA-PDT efficacy on TNBC in a simulated hormonal microenvironment.

Approach: The 3D spheroids of TNBC cells (MDA-MB-231) were generated in the hormonal supplemented microenvironment. The accumulation of PpIX, phototoxicity, the ROS level and p-ULK1 expression level mediated by Hexyl-ALA-PDT were determined by confocal microscopy, MTT assay and flow cytometry.

Results: A lower Hexyl-ALA concentration was required to achieve the same lethal dose of LD50 with hormonal supplement in 3D spheroids. It was found that the ROS level was increased at lower Hexyl-ALA-PDT dose in hormonal microenvironment, which also correlated the decrease of p-ULK1 expression by PDT.

Conclusions: Hexyl-ALA-PDT increased ROS level in TNBC in hormonal microenvironment; and with the reduced p-ULK1 expression thus indicating autophagy of cell death might be triggered.

Keywords: Photodynamic Therapy, Triple Negative Breast Cancer, Hormonal microenvironment, 3D spheroids, Hexyl-ALA

1. Introduction and Background

Cancer cell growth can be facilitated by hormones normally present in the physiological microenvironment [1,2,3]. Studies usually focused on cancer treatment effect with only a single dose of hormone, such results over-estimated the treatment efficacy and ignored the hormonal effect on the treatment efficacy in normal physiological tumor microenvironment [4, 5]. Our pilot studies evidenced the hormonal enhancement of photodynamic therapy (PDT) efficacy in hormonal dependent cancers